Atomic and electronic structure of GaP/Si(111), GaP/Si(110), and GaP/Si(113) interfaces and superlattices studied by density functional theory

O. Romanyuk*
Institute of Physics, Academy of Sciences of the Czech Republic, Cukrovarnická 10, 16200 Prague, Czech Republic

T. Hannappel
Ilmenau University of Technology, Institute of Physics, 98684 Ilmenau, Germany and
CiS Forschungsinstitut für Mikrosensorik und Photovoltaik GmbH, Konrad-Zuse-Straße 14, 99099 Erfurt, Germany

F. Grosse
Paul-Drude-Institut für Festkörperelektronik, Hausvogteiplatz 5–7, 10117 Berlin, Germany
(Received 23 April 2013; revised manuscript received 18 July 2013; published 23 September 2013)

The atomic structure of GaP(111)/Si(111), GaP(110)/Si(110), and GaP(113)/Si(113) heterointerfaces was studied by *ab initio* calculations employing the density functional theory (DFT). Relative formation energies were computed for the interface layers allowing for atomic intermixing. The application of the electron-counting model, a construction principle used for surface reconstructions, to the case of the GaP(111)/Si(111) interfaces leads to electronic compensation at the heterovalent interfaces and to a reduction of the interface formation energy. The specific equilibrium (111) interface reconstruction can be tuned by changing the chemical potential. In particular, the GaP(111)A/Si(111) interface was found to be abrupt and uncompensated under P-rich conditions, whereas it is compensated under Ga-rich conditions. The GaP(111)B/Si(111) interface was found to be compensated. Contrary to the (111) interfaces, stoichiometric abrupt interfaces were found to be the most energetically favorable for the GaP(110)/Si(110) and the GaP(113)/Si(113) interfaces. These interfaces do not reconstruct. Although both interfaces are compensated, the GaP(113)/Si(113) superlattice exhibits a polarization field, in contrast to the (110) superlattice.

DOI: 10.1103/PhysRevB.88.115312 PACS number(s): 68.35.Ct, 79.60.Jv, 73.40.Kp

I. INTRODUCTION

The heteroepitaxial growth of group III-V materials on Si substrates opens up new application perspectives. It allows the monolithic integration of semiconductor devices such as infrared lasers, detectors, solar cells, and transistors into complex silicon integrated circuits. The performance of devices containing thin epitaxially grown layers depends on the quality of the layers and, particularly, on the quality of the interface between the device layers. The interface itself is influenced by the lattice and the electronic structure of the adjacent materials. A close lattice constant match is desirable in order to avoid defect formation due to lattice relaxation. By combining III-V materials with Si, another fundamental issue is important, which results from the differences in the electronic bond configuration.

GaP is an attractive candidate for complementary metal-oxide-semiconductor (CMOS) technology since it is almost lattice matched to Si. Crystalline GaP films can be grown on Si(001),[1–3] Si(111), Si(110), and Si(113)[4–6] substrates by metalorganic chemical vapor deposition (MOCVD). Although a number of growth-technology questions related to the reduction of the antiphase domain boundary defects for (001) facets[7–9] and twin defects for (111) faces[5] still remain open, well-ordered GaP/Si heterostructures have already been grown.

For closely lattice matched heterostructures, as is the case for the GaP/Si system, elastic contributions are negligible. Instead, the electronic mismatch becomes the essential ingredient: an electronic bond configuration diversity of heterovalent atoms at the interface plays a crucial role for the creation of an abrupt and sharp interface.[10,11] An excess or deficiency of electrons in the atomic bond configurations of electronically dissimilar materials directly influences the quality and electronic properties of the epitaxial layers.

In the present paper, we investigate the interface structure and electronic charge compensation mechanism for lattice-matched (coherent) but electronically mismatched (heterovalent) GaP/Si interfaces. The electronic mismatch at the interface is discussed in the framework of the electron-counting model (ECM), which was originally suggested for semiconductor surfaces.[12] The ECM postulates a charge redistribution between the group III and V dangling bonds at surfaces by emptying the energetically higher-lying group III bonds and filling the group V bonds completely.[13,14] Transferring the ECM to the GaP/Si interface situation suggests a necessary exchange of electrons between the Ga-Si bonds with an electron deficiency and the P-Si bonds with an electron excess at the interface. This exchange could arise within the same interface or between neighboring interfaces in a superlattice (SL) if the distance between the interfaces is not too large. An interface fulfills the ECM if the total number of excess electrons from the P-Si bonds equals the number of deficient electrons in the Ga-Si bonds. Such interfaces will be called "compensated" in the following text. Closely related are the resulting polarization fields originating in the formed dipole layers at the heterointerfaces. These are essential, e.g., to interpret the electronic properties in a SL.[15]

Electronic compensation between different bond types at coherent heterovalent interfaces can be realized by varying the atomic stoichiometry within the interface layers. It was

shown that an atomic mixture within two interface layers can compensate the heterovalent bonds and even remove a dipole shift of the averaged electrostatic potential in GaAs/Ge(001) heterostructures.[16] The dipole shift is eliminated by an interfacial atomic plane consisting of 3/4 Ga and 1/4 As atoms per (2 × 2) cell. It was also shown that a dipole shift depends on the atomic stoichiometry at the interface rather than on the details of the atomic arrangement within the transition layers.

The heterointerface formation energies of zincblende[17–20] and wurtzite[21] semiconductor superlattices were investigated by *ab initio* calculations. The uncompensated coherent interfaces were found to be energetically unfavorable, whereas an atomic mixture between heterovalent species reduced the interface energy. It was additionally shown that a dipole shift elimination at the interface is not a necessary condition for the lowest-energy interface structure: models with two mixed layers, which realize a vanishing dipole moment, were found to be less energetically favorable than models with only one mixed layer.[20]

In the present paper, the interface structures of the GaP/Si(111), the GaP/Si(110), and the GaP/Si(113) heterostructures are investigated by *ab initio* calculations. Total energies as a function of the chemical potential at the interface are calculated for interface models with a (2 × 2) and a $c(4 \times 2)$ unit cell for the (111) SL and with (1 × 1) cells for the (110) and (113) SL. Relative interface formation energy diagrams reveal differences in the GaP/Si interface stabilization along different directions.

II. COMPUTATIONAL DETAILS

Ab initio calculations of the relative formation energies were carried out using the ABINIT computer code.[22,23] The generalized gradient approximation (GGA) for the exchange-correlation energy functional was used. Norm-conserving pseudopotentials[24] of the Troullier-Martins type[25] were used to describe the atomic species. The electronic wave functions were expanded in a plane-wave basis with a converged kinetic-energy cutoff of 12 Hartree (Ha). The **k**-point sets[26] corresponding to $5 \times 5 \times 1, 8 \times 10 \times 1, 7 \times 10 \times 1$ points per (2 × 2)-(111), (1 × 1)-(110), and (1 × 1)-(113) SL Brillouin zones, respectively, were used. Periodic boundary conditions were applied along the in-plane and out-of-plane directions.

A SL slab consists of 24 bilayers (12 bilayers for Si and 12 for GaP, 12-12) for (111), 12-12 bilayers for (110), and 11-11 bilayers for (113) superlattices. The converged SL thickness was estimated by gradually increasing the slab thickness and by computing the interface total-energy differences between two slabs with different thicknesses.[20]

Equilibrium lattice constants were computed for bulk Si ($a_{\mathrm{Si}} = 5.46$ Å) and GaP ($a_{\mathrm{GaP}} = 5.50$ Å). The atomic positions were adjusted until the interatomic forces became smaller than 10^{-3} Ha/Bohr. In order to compensate for the elastic strain arising due to the calculated difference in GaP/Si lattice constants, the unit cell translation vectors were allowed to relax. The relaxed SL size difference was found to be less than 0.08 Å along the Z direction and 0.1 Å along the in-plane directions per SL.

A (111) SL consists of two interfaces that have a type A (Si-P) or type B (Si-Ga) polarity. We investigated the stability of one interface as a function of the chemical potential, keeping the second interface fixed in a reference configuration. The relative interface formation energy $\Delta\gamma$ is defined as[20,21]

$$\Delta\gamma A = E_{\mathrm{tot}} - \Sigma_i n_i \mu_i, \tag{1}$$

where E_{tot} is the total energy of a slab, μ_i is the chemical potential of species i, n_i is the number of atoms of the species i, and A is the interface unit cell area. In thermodynamic equilibrium the chemical potentials are equal to the bulk chemical potentials μ_i^{bulk}:

$$\mu_{\mathrm{GaP}}^{\mathrm{bulk}} = \mu_{\mathrm{Ga}} + \mu_P, \tag{2}$$

$$\mu_{\mathrm{Si}}^{\mathrm{bulk}} = \mu_{\mathrm{Si}}. \tag{3}$$

In particular, the μ_{Ga} and μ_P chemical potentials depend on the experimental conditions, i.e., the substrate temperature and the atomic flux. Their values are limited to the bulk chemical potential values of element i; otherwise, Ga or P bulk phases would form. Thus, the boundary conditions for the chemical potential variation can be expressed as

$$H_f^{\mathrm{GaP}} \leqslant \Delta\mu_P \leqslant 0, \tag{4}$$

$$\Delta\mu_P = \mu_P - \mu_P^{\mathrm{bulk}}, \tag{5}$$

$$H_f^{\mathrm{GaP}} = \mu_{\mathrm{GaP}}^{\mathrm{bulk}} - \mu_{\mathrm{Ga}}^{\mathrm{bulk}} - \mu_P^{\mathrm{bulk}}, \tag{6}$$

where H_f^{GaP} is the heat of formation and μ_i^{bulk} is the bulk chemical potential of the ith element. The corresponding bulk chemical potentials were calculated for the orthorhombic α-Ga phase[27] and the orthorhombic black phosphorous[28] phase with an energy cutoff of 12 hartrees. The GaP heat of formation[29] $H_f^{\mathrm{GaP}} = -0.91$ eV was derived.

In addition to varying the Ga and P chemical potentials, the Si chemical potential can also be varied at the interface. Although the Ga and P elements do not form silicides, a pyrite SiP_2 compound potentially could be formed.[30,31] Nevertheless, the SiP_2 heat of formation $H_f^{\mathrm{SiP_2}} = -0.42$ eV was found to be larger than H_f^{GaP}. Thus, GaP bulk-phase formation is preferred compared to SiP_2 in a GaP/Si heterostructure. By substituting Eqs. (2), (3), and (6) into Eq. (1), the relative interface formation energy $\Delta\gamma$ is expressed as

$$\Delta\gamma A = E_{\mathrm{tot}} - (n_P - n_{\mathrm{Ga}})\Delta\mu_P - n_P\mu_{\mathrm{GaP}}^{\mathrm{bulk}} - n_{\mathrm{Si}}\mu_{\mathrm{Si}}^{\mathrm{bulk}}. \tag{7}$$

It should be emphasized that γ involves contributions from two interfaces present in the SL. The absolute interface energy formation can be derived by a local energy density integration for abrupt interfaces.[19] In our study, however, we use the relative interface formation energies since these are sufficient for structure discrimination.

III. RESULTS AND DISCUSSION

A. (111) interfaces

A GaP/Si(111) SL is depicted in Fig. 1(a). The slab contains 12 GaP bilayers and 12 Si bilayers (the Si layers were truncated in the figure for convenience). The interface in-plane unit cell has been chosen to have a (2 × 2) size since this is the smallest cell size for which the ECM can be fulfilled. The SL consists of

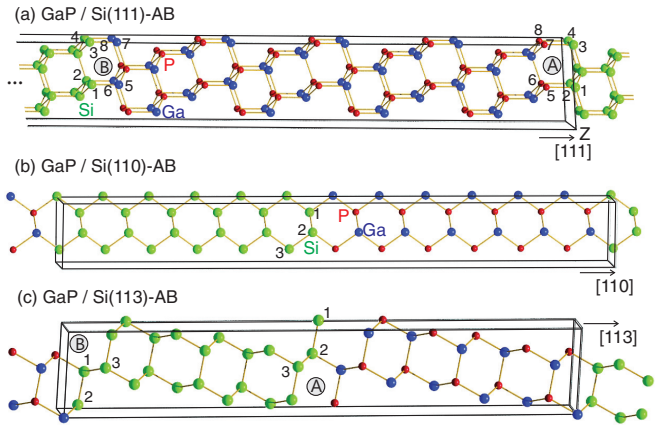

FIG. 1. (Color online) Structure models of the (a) GaP/Si(111)-(2 × 2), (b) GaP/Si(110)-(1 × 1), and (c) GaP/Si(113)-(1 × 1) superlattices. The green, blue, and red atoms correspond to Si, Ga, and P atoms, respectively. A (111) cell in (a) was cut from the left-hand side. A (111) SL consists of type A (P-Si) and type B (Ga-Si) interfaces, whereas both interfaces are equivalent in (b). Substitutional site positions are marked by numbers.

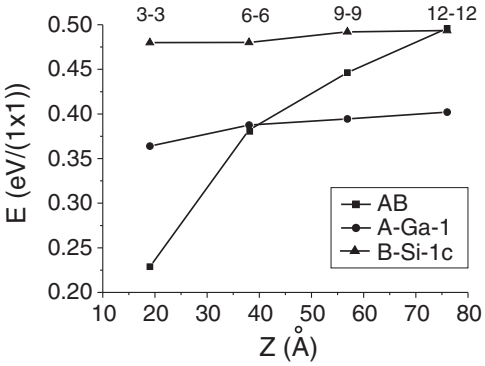

FIG. 2. Total interface energy as a function of supercell thickness Z for abrupt A and B interfaces (AB) and for one compensated and one abrupt interface in the SL, A-Ga-1 for A polarity and B-Si-1c for B polarity. The total energy contains contributions from both interfaces. Si-GaP slab thicknesses of up to 12-12 bilayers are used in the calculations.

a type A and a type B interface. Possible substitutional atomic sites are marked by indexes 1–8 at the A and B interfaces in Fig. 1(a). The model notation AB refers to a SL with two abrupt stoichiometric interfaces. The model notation B-Si-567, for instance, denotes a model with a chemical potential variation at interface B, where Si atoms substitute atoms at sites 5, 6, and 7.

There are electrostatic and elastic interactions between the A and B interfaces in a SL. In order to reduce interface interaction, a sufficiently large SL periodicity is necessary. Electrostatic contributions to the SL total energy increase linearly with SL thickness, similar to the capacitor energy. Stress originates at the interface due to the formation of bonds with a length deviating from the lattice constants of GaP and Si. This interface stress is relaxed in a superlattice perpendicular to the interface and is therefore localized at the interface region.

The interface energy dependence on the (111)-AB SL thickness was computed. A gradual increase of the SL thickness leads to a decrease of the interface energy difference similar to the (001) SL.[20] In Fig. 2, the total interface energy as a function of the SL thickness for different interface structures in a slab is shown. The energy E contains contributions from the A-type and B-type interfaces. These two interfaces are present in the SL simultaneously. The difference in the interface energy decreases with the SL thickness. For slabs with an A-type or B-type compensated interface, the total-energy convergence occurs for smaller thicknesses than in the case of uncompensated interfaces, AB. A difference in the interface energy of less than 10 meV/(1 × 1) by adding another bilayer is assumed to be sufficient. The energy variation between Si-GaP slab thicknesses of 13-11 or 11-13 is less than 5 meV/(1 × 1) unit cell. Slab thicknesses of 12-12, 12-12, and 11-11 GaP-Si bilayers were used for (111), (110), and (113) SL calculations, respectively.

The GaP/Si interfaces are heterovalent since they involve group IV and group III (V) bonding configurations. A covalent bond of bulk Si and GaP requires two electrons per bond. Each Si atom contributes one valence electron per bond, whereas Ga (P) provides 3/4 (5/4) valence electrons per bond. A Ga-Si (P-Si) bond therefore has a 1/4 electron deficiency (1/4 excess) per covalent bond.

An atomic mixture within an interface layer is a possible way to fulfill the ECM at a heterovalent III-V/IV interface. For instance, the abrupt GaP(111)A/Si(111) interface with Si-P bonds would have a one-electron excess per (2 × 2) cell [AB model in Fig. 1(a)]. In order to fulfill the ECM, electronic states with a one-electron deficit are required. Such a structure can be realized by introducing one substitution site of dissimilar atoms with a different valence within a (2 × 2) cell. By substituting a Ga atom for a Si atom at site 1 for the A interface of the AB model, the interface fulfills the ECM. The A-Ga-1 model with one substitutional site per (2 × 2) cell consists of three P-Si and three Ga-Si bonds with partial charges of $-0.75e$ and $0.75e$, respectively. Thus, this configuration leads to a compensated interface. The unit cell with a (2 × 2) unit cell area is the smallest for which the ECM can be fulfilled. Larger cell areas with a multiple of four (1 × 1) cells are also possible.

In the present paper, the relative formation energies were computed for the heterovalent interfaces with (2 × 2) and $c(4 \times 2)$ unit cells. These cells have the same area. The atomic arrangement in the centered cells was considered to be similar to the corresponding arrangement in the (2 × 2) cell. The in-plane unit cell translations are different, however: the centered cells are shifted (2 × 2) cells by one surface lattice constant a_s relative to each other.[32,33]

The following atomic substitution sites within the interface unit cell were considered. For the (111)-A (B) interface, Si atoms can substitute for P (Ga) atoms at sites 5–8, and Ga (P) atoms can substitute for Si atoms at sites 1–4 [Fig. 1(a)]. The A-Ga-1, A-Si-5, B-P-1, and B-Si-5 models with one substitutional site fulfill the ECM for both (2 × 2) and $c(4 \times 2)$ (denoted by "c") cells. In Figs. 3(a) and 3(b) calculated relative formation energy diagrams are shown for (111)A and (111)B interfaces, respectively. Since the reference interfaces in a slab are different for (111)A and (111)B interfaces, a direct comparison of the A and B relative interface energies is not

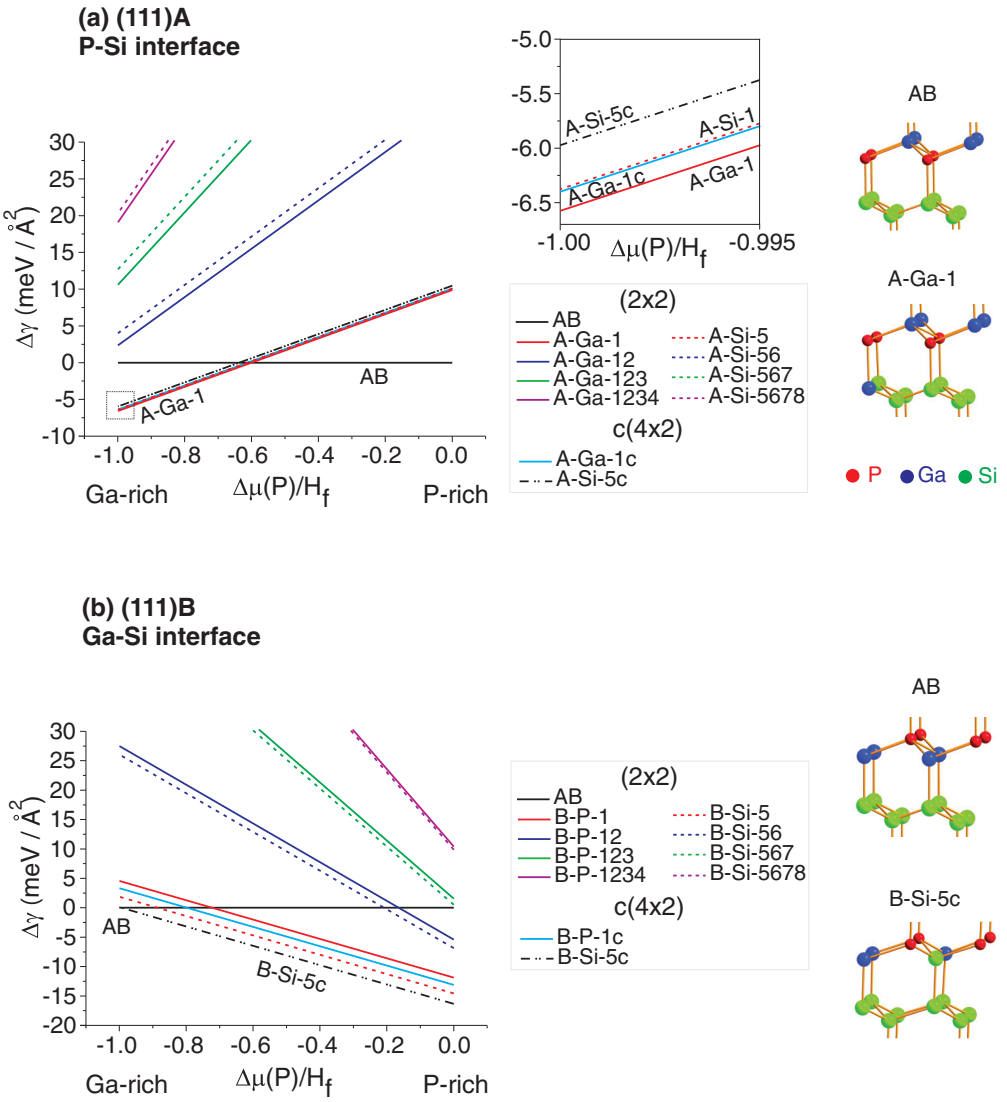

FIG. 3. (Color online) Relative interface formation energy diagrams for (a) GaP(111)A/Si(111) and (b) GaP(111)B/Si(111) interfaces. The model notation contains the interface type and the substitutional-site positions according to Fig. 1. A "c" in the model notation denotes centered $c(4 \times 2)$ unit cells. The energy is given in meV/Å^2. The energy of the abrupt, unreconstructed SL was chosen as the reference and was set to zero.

possible. Hence, the reported values are to be interpreted as relative energies for the different atomic interface structures.

We found the following results.

(i) The P-Si interface is compensated under Ga-rich conditions [Fig. 3(a)]. The A-Ga-1 (2×2) structure model with one substitutional Ga site has the lowest interface energy. Other compensated models such as A-Ga-1c, A-Si-1, and A-Si-5c structures with one substitutional site are very close in energy. In Fig. 3(a), a magnified region close to $\Delta\mu(P)/H_f = -1.0$ is shown for compensated interfaces. The energy difference between the compensated models is lower than 0.65 meV/Å^2. Small energy differences between structures in the ground state can be overcome by configurational entropy contributions at an elevated temperature.[13] The uncompensated P-Si interface models with more than one substitutional site per (2×2) or $c(4 \times 2)$ cell are higher in energy and can be ruled out.

(ii) The P-Si interface is abrupt under P-rich conditions. The interface is uncompensated in thermodynamic equilibrium.

(iii) For the P-Si interface, structures with Ga substitutional sites [solid lines in Fig. 3(a)] are more energetically favorable than structures with Si substitutional sites (dashed lines). For the Ga-Si interface, the Si substitutional sites are energetically more favorable than the P substitutional sites. Thus, the Ga/Si atomic intermixture is more energetically favorable than the P/Si intermixture at interfaces with both polarities.

(iv) The Ga-Si interface is predicted to be reconstructed and compensated under P-rich conditions. The most energetically favorable B-Si-5c structure has one Si substitutional site in the Ga layer and fulfills the ECM. Structures with P substitutional sites have higher energy and are unfavorable. The B-Si-5c structure with $c(4 \times 2)$ cell has a smaller energy than the B-Si-5 structure with a (2×2) cell by 0.7 meV/Å^2. For a (111)A compensated interface, models with centered translation periodicity have higher energy than their counterpart models with the (2×2) cells. We speculate that an interplay between the Madelung energy contribution[20,34]

and stress contributions to energy due to substitution sites at the interface could take place. It should be mentioned that due to the small energy difference between oblique and rectangular cells, the coexistence of both structures is possible at an elevated temperature,[13] i.e., random substitution site distribution in the interfacial layers. Under such conditions it would be challenging to determine the interface periodicity by x-ray diffraction; for instance, the specific x-ray fractional order peak maxima that would indicate a long-range order due to an interface reconstruction would be suppressed if a Bravais lattice diversity occurs.[35]

For a GaP/Si epitaxial film, the energy of a reference interface in the SL has to be replaced by the surface formation energy. If GaP surface reconstructions fulfill the ECM, the GaP surfaces can be considered to be compensated. Although epitaxial films have not been considered in the current paper, the reliability of the results obtained for SL was verified with respect to a compensated reference interface. The compensated B-Si-5 interface was set as a reference interface, whereas the stoichiometry was varied at the (111)A interface. We confirmed that compensated GaP(111)A/Si(111) interface models have a lower energy compared to uncompensated interface models in this case. Thus, the results for the SL could also be used for thin epitaxial films.

From the present results of relative (111) interface energies, it is not possible to conclude which interface polarity is more favorable under specific experimental conditions, but the thermodynamically stable interface structures are determined for isolated GaP/Si interfaces. Specifically, for P-rich conditions, the A-type interface is predicted to be abrupt; that is, no Ga/Si intermixture takes place in equilibrium. In contrast, the Si/Ga intermixture is favorable for interfaces with B-type polarity.

Valence electron density maps of the atomic plane through the Si substitution site perpendicular to the GaP/Si interface are shown in Fig. 4. The atomic plane of the relaxed B-Si-5c model is schematically shown in Fig. 4(a): there is a Si substitution site at the interface marked by a green arrow. The relaxed bond lengths between the Si-Ga and Si-Si atoms were found to be equal in the interfacial layer. A cross-sectional view of the corresponding valence electron density map is presented in Fig. 4(b). Atomic positions are indicated by the corresponding spheres. The localized bond electrons lead to high electron densities. The higher electronegativity of the P atoms leads to a higher electron density in their vicinity. A Si substitution site at the interface is indicated by a green arrow in Fig. 4(b). No significant difference in the valence electron density is observed around the Si substitution site due to charge transfer at the compensated interface.

Electrostatic interactions between the interfaces in the relaxed SL were deduced from the averaged Hartree potential. The potential was averaged in plane (XY) over the interface unit cell area and plotted along the [111] (Z) direction.[20] The P-Si and Si-Ga interfaces in a slab are situated at 37 Å and 75 Å from the origin. In Fig. 5(a), the averaged Hartree potential is given for the relaxed uncompensated (111)-AB model. Additionally, the Z average over the atomic layer of the potential is indicated by a red line. The tilt of the averaged potential reflects the polarization field originating from the interface dipoles.

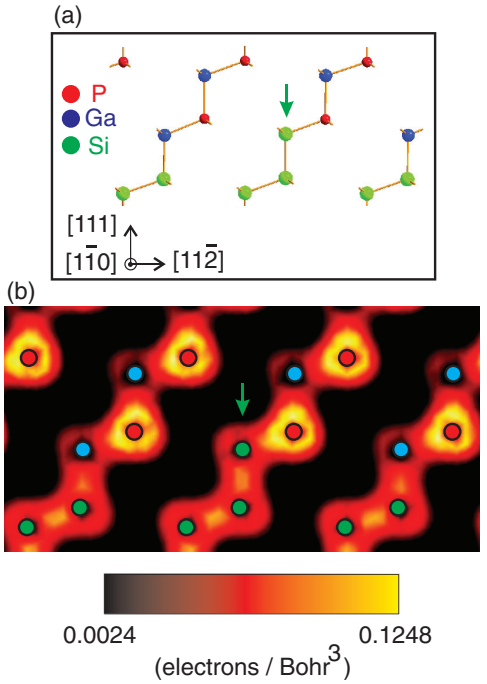

FIG. 4. (Color online) (a) The relaxed atomic plane of the Ga-Si interface of the B-Si-5c structure. The Si substitution site is indicated by a green arrow. (b) Valence electron density cross-sectional map of the corresponding plane. Atomic positions are shown by red, blue, and green spheres for P, Ga, and Si atoms, respectively. There is no significant difference in the valence electron density for the Si substitution site (marked by an arrow).

In Figs. 5(b) and 5(c), the averaged Hartree potentials of the A-Ga-1 and B-Si-5 structures are shown. The potentials and electron densities of the SL with $c(4 \times 2)$ and (2×2) cells were found to be equivalent, and only the potentials and densities of the (2×2) cells are plotted in Fig. 5. There are compensated and uncompensated (reference) interfaces in the SL in Figs. 5(b) and 5(c). Despite the charge compensation on one interface only, the internal polarization field was reduced significantly: the averaged electrostatic potentials are aligned almost horizontally in the SL. Small deviations from the horizontal plane are caused by the small residual dipole differences at the interfaces.

The average number of valence electrons ρ_{av} per bilayer along the [111] direction is shown in Figs. 5(d)–5(f) for AB, A-Ga-1, and B-Si-5 structures, respectively. The unrelaxed interplanar bilayer distances of 3.16, 1.93, and 1.52 Å were used for the electron density integration for the (111), (110), and (113) superlattices, respectively. Similar to the Hartree potential, the electron density was averaged. The red lines represent the Z average over the atomic layer of the valence electron density ρ. The valence electron density shows a significant variation at the interfaces compared to the bulk values. Compensated interfaces are marked by yellow arrows in Figs. 5(e) and 5(f). There are small deviations of the valence electron density due to atomic intermixture (indicated by arrows) with respect to uncompensated interfaces.

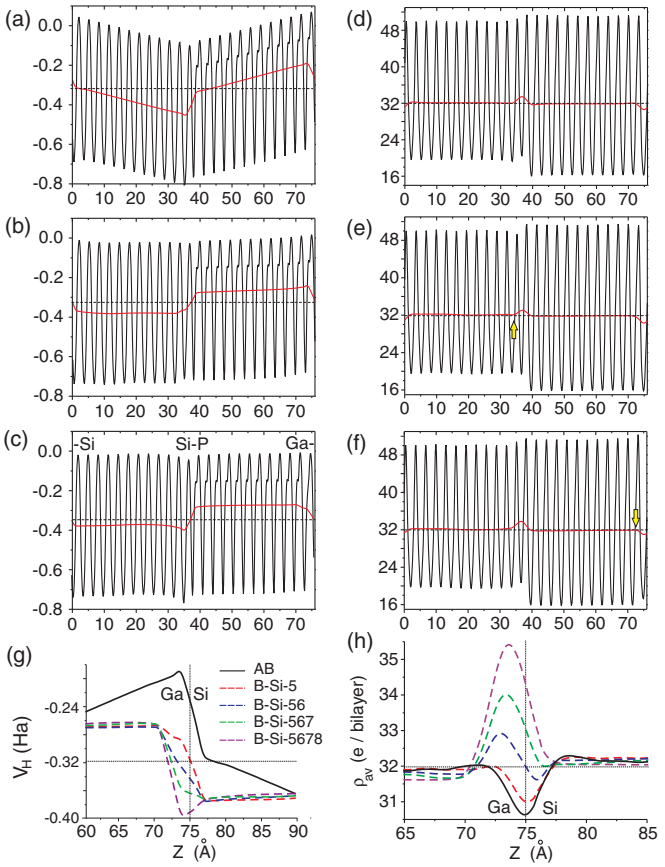

FIG. 5. (Color online) Averaged electrostatic potential V_H of the (a) AB, (b) A-Ga-1, and (c) B-Si-5 superlattices. The averaged number of electrons per bilayer along the (111) direction is shown for (d) AB, (e) A-Ga-1, and (f) B-Si-5 interface structures. The Si-P and Si-Ga interfaces lie at 37 Å and 75 Å, respectively. The Ga-Si interface region is magnified in (g) and (h) for a structure with Si chemical potential variation at the interface. The Hartree potential shape and electronic charge density shape at the interface vary with atomic stoichiometry.

A magnified region of the averaged Hartree potentials and electronic charge density are shown in Figs. 5(g) and 5(h) for B-Si-5 structures with different stoichiometry at the Si-Ga interface. There are 32 valence electrons present in the Si and GaP bulk bilayer. A small deviation from this number in Fig. 5(h) is due to atomic plane relaxations. A gradual change of potentials and electronic charge density with varying Si stoichiometry is seen. A similar behavior was observed for the Si-P interfaces (not shown here). The red dashed lines in Figs. 5(g) and 5(h) correspond to the most energetically favorable structures with a compensated interface. Substitutional-site defects influence the electrostatic field in the SL.

B. (110) and (113) interfaces

Epitaxial layers of GaP(110) and GaP(113) can be grown on Si substrates with the corresponding crystal orientations. The epitaxial film quality grown on (110) and (113) substrates was found to be better than the (111) film quality.[4,5] The (110) and (113) GaP/Si interfaces consist of heterovalent Ga-Si and P-Si bonds within a (1×1) interface cell. From the ECM point of view, such interfaces are compensated: the number of P-Si bonds per (1×1) cell is equal to the number of Ga-Si bonds in the interfacial layer. An atomic mixture at the (110) interface would bring additional defects and would increase the interface energy.

In Figs. 1(b) and 1(c), the GaP/Si(110) and GaP/Si(113) (1×1) SL structure models are shown. For the (110) SL, the Ga-P dimer lies parallel to the interface plane. The number of anion atoms is equal to the number of cation atoms in the (1×1) interface cell. In the (113) SL, however, the Ga-P atomic dimers are tilted with respect to the interface plane [Fig. 1(c)].

The in-plane unit cell translation vector lengths are $a_s^{110} = 5.46$ Å, $b_s^{110} = 3.86$ Å and $a_s^{113} = 6.66$ Å, $b_s^{113} = 3.86$ Å for the (110) and (113) (1×1) unit cells, respectively. The angle between the a_s^{113} and b_s^{113} vectors is 73.22°. Slabs consisting of 12-12 atomic bilayers for the (110) SL and 11-11 bilayers for the (113) SL [Figs. 1(b) and 1(c)] were used in the calculations. In the (113) SL case, the particular number of layers produces a monoclinic SL cell. The relative total energies of the (110) and (113) interfaces with different stoichiometry have been computed.

In Fig. 6(a), the phase diagram is shown for the (110) SL. The total energy of the abrupt stoichiometric SL is used as the

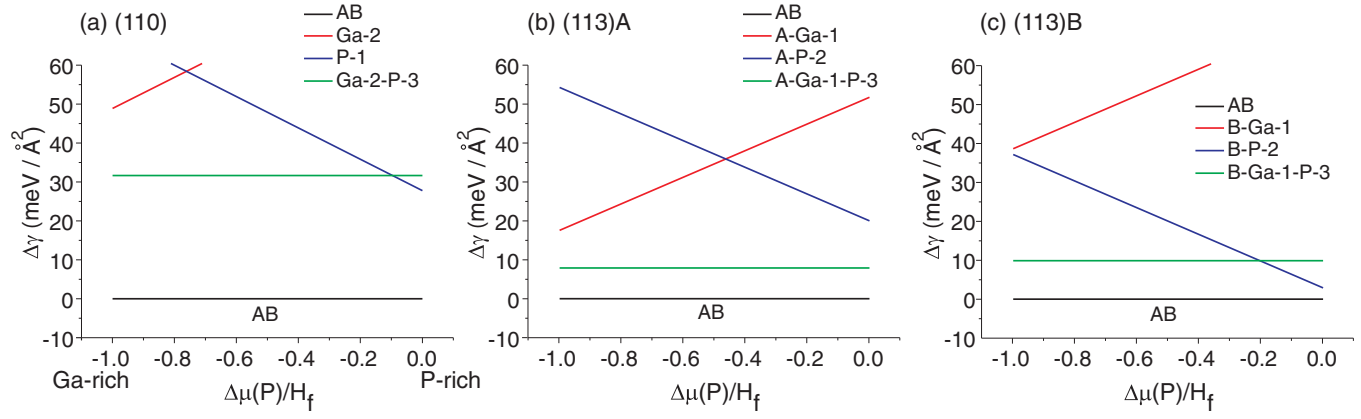

FIG. 6. (Color online) Relative interface formation energy diagrams for (a) GaP(110)/Si(110), (b) GaP(113)A/Si(113), and (c) GaP(113)B/Si(113). Abrupt stoichiometric interfaces are confirmed for the (110) and (113) superlattices.

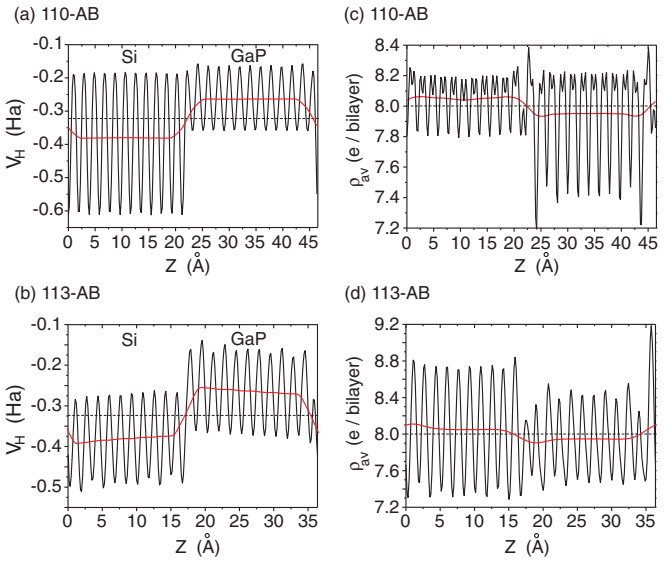

FIG. 7. (Color online) Averaged electrostatic potential V_H of the (a) (110) and (b) (113) superlattices. The stoichiometric interfaces are compensated. Spontaneous electric polarization in the (113)-AB SL caused the tilt of V_H in (b). The averaged electronic charges for (110) and (113) SLs are shown in (c) and (d), respectively.

reference energy level (set to zero). Ga and P substitutional sites were introduced at the interface according to the site specification in Fig. 1(b). The substitutional sites make the (110) interface uncompensated. We found that the abrupt stoichiometric (110) interface with a (1×1) cell has the smallest energy. Thus, the nonpolar GaP/Si interface is stable against atomic intermixture.

In Figs. 6(b) and 6(c), the relative energy phase diagrams are shown for the (113)A (P-Si) and (113)B (Ga-Si) interfaces. Similar to the (110) interface, the stoichiometric compensated (113) interface was found to be the most energetically stable, as expected. However, the energy difference between the compensated interfaces and the interfaces with atomic substitutional sites is smaller for the (113) interface than for the (110) interface. The (110) interface is more stable against substitutional-site defects.

In Figs. 7(a) and 7(b), the averaged Hartree potential is shown for (110)-AB and (113)-AB structures. There is no electric field in the (110) SL: both interfaces in the slab are compensated. A valence band offset (VBO) of 0.5 eV is computed for the GaP/Si(110) superlattice. This value is close to the value given in the literature for superlattices[36] (VBO = 0.55 eV) and GaP/Si(110) epitaxial films[37] (VBO = 0.45 eV). In contrast to the (110) GaP SL, the (113) SL contains a finite gradient of the averaged Hartree potential V_H (red line) in Fig. 7(b), although all of the interfaces are compensated. The origin of the field for the (113) SL is a residual interface dipole due to relaxations within the interface plane.

For the (111) SL, a slab with two compensated A-Ga-1 and B-Si-1 interfaces was used for VBO calculation to avoid a finite gradient of the averaged Hartree potential. Our computed value for SL consisting of A-type and B-type GaP/Si(111) interfaces is VBO = 0.76 eV. This is close to the computed value for the GaP(111)/Si epitaxial films (0.88 eV)[38] but quite different from the VBO of the GaP($\bar{1}\bar{1}\bar{1}$)/Si film (0.97 eV).[38] Detailed experimental studies of the VBO of the GaP/Si(111) superlattices are still required.

The averaged electron densities of the compensated (110) and (113) SLs are shown in Figs. 7(c) and 7(d), respectively. Similar to Fig. 5, the black curves correspond to the averaged electron density within the XY plane, whereas the red curves are the Z-averaged electron densities. Interplanar relaxations of the Si layers are responsible for the slight deviations of the horizontal alignment in Fig. 7(c). Nevertheless, smooth electron density variations without charge accumulation have been confirmed for (110) and (113) interfaces.

Finally, the abrupt stoichiometric (110) and (113) GaP/Si heterointerfaces were found to be energetically more favorable than the interfaces with atomic intermixture. The (110) and (113) GaP/Si heterointerfaces do not reconstruct. The GaP/Si(110) SL does not show a polarization field, whereas it is present in the GaP/Si(113) superlattice.

IV. CONCLUSIONS

The interface structures of GaP/Si superlattices with (111), (110), and (113) orientations have been investigated by *ab initio* calculations. The relative interface formation energies of the Ga-Si and Ga-P interfaces with atomic intermixture in the interfacial layers have been compared. We found, depending on the chemical potential, that heterovalent interfaces can reconstruct by allowing atomic intermixing within the interfacial layers. The reconstructed compensated interfaces are energetically favorable for GaP(111)A/Si(111) under Ga-rich conditions, whereas an abrupt and uncompensated interface is favorable under P-rich conditions. The GaP(111)B/Si(111) interface is compensated over the whole chemical potential range. Atomic intermixture is expected at these interfaces. Thus, the GaP(111)/Si(111) interfaces with A- and B-type polarities do stabilize differently. Electronic charge compensation at polar interfaces is realized by charge redistribution within the interfacial layers. Chemical potential variation in the interfacial layers could be useful for valence-band offset engineering for device fabrication. The GaP/Si(110) and GaP/Si(113) interfaces do not reconstruct, and atomic intermixture is not favorable for these interfaces. A polarization field was found for the GaP/Si(113) superlattice, whereas none is present in the GaP/Si(110) superlattice.

ACKNOWLEDGMENTS

This work was supported by the Grant Agency of the Czech Republic (Project No. P204/10/P028) and the Academy of Sciences of the Czech Republic (Project No. M100101201). The access to the MetaCentrum computing facilities provided under Project No. LM2010005 funded by the Ministry of Education, Youth, and Sports of the Czech Republic is highly appreciated. Part of this work was supported by the BMBF (Project No. 03SF0404A) and by the German Research Foundation (DFG, Project No. HA 3096/4).

*romanyuk@fzu.cz

[1] F. Ernst and P. Pirouz, J. Appl. Phys. **64**, 4526 (1988).
[2] K. J. Bachmann, U. Rossow, N. Sukidi, H. Castleberry, and N. Dietz, J. Vac. Sci. Technol. B **14**, 3019 (1996).
[3] H. Döscher, B. Borkenhagen, G. Lilienkamp, W. Daum, and T. Hannappel, Surf. Sci. **605**, L38 (2011).
[4] V. Narayanan and S. Mahajan, Philos. Mag. A **80**, 555 (2000).
[5] V. Narayanan, S. Mahajan, K. J. Bachmann, V. Woods, and N. Dietz, Philos. Mag. A **82**, 485 (2002).
[6] N. Sukidi, K. J. Bachmann, V. Narayanan, and S. Mahajan, J. Electrochem. Soc. **146**, 1147 (1999).
[7] H. Döscher, T. Hannappel, B. Kunert, A. Beyer, K. Volz, and W. Stolz, Appl. Phys. Lett. **93**, 172110 (2008).
[8] H. Döscher, B. Kunert, A. Beyer, O. Supplie, K. Volz, W. Stolz, and T. Hannappel, J. Vac. Sci. Technol. B **28**, C5H1 (2010).
[9] H. Döscher, T. Hannappel, O. Supplie, S. Brückner, A. Beyer, and K. Volz, J. Cryst. Growth **315**, 16 (2011).
[10] D. M. Bylander and L. Kleinman, Phys. Rev. B **41**, 3509 (1990).
[11] N. Nakagawa, H. Y. Hwang, and D. A. Muller, Nat. Mater. **5**, 204 (2006).
[12] M. D. Pashley, Phys. Rev. B **40**, 10481 (1989).
[13] O. Romanyuk, F. Grosse, A. Proessdorf, W. Braun, and H. Riechert, Phys. Rev. B **82**, 125315 (2010).
[14] A. Proessdorf, F. Grosse, W. Braun, F. Katmis, H. Riechert, and O. Romanyuk, Phys. Rev. B **83**, 155317 (2011).
[15] A. Franciosi and C. G. V. de Walle, Surf. Sci. Rep. **25**, 1 (1996).
[16] W. A. Harrison, E. A. Kraut, J. R. Waldrop, and R. W. Grant, Phys. Rev. B **18**, 4402 (1978).
[17] D. B. Laks and A. Zunger, Phys. Rev. B **45**, 14177 (1992).
[18] N. Chetty and R. M. Martin, Phys. Rev. B **45**, 6074 (1992).
[19] N. Chetty and R. M. Martin, Phys. Rev. B **45**, 6089 (1992).
[20] A. Kley and J. Neugebauer, Phys. Rev. B **50**, 8616 (1994).
[21] J. von Pezold and P. D. Bristowe, J. Mat. Sci. **40**, 3051 (2005).
[22] X. Gonze, J.-M. Beuken, R. Caracas, F. Detraux, M. Fuchs, G.-M. Rignanese, L. Sindic, M. Verstraete, G. Zerah, F. Jollet *et al.*, Comput. Mater. Sci. **25**, 478 (2002).
[23] X. Gonze, G.-M. Rignanese, M. Verstraete, J.-M. Beuken, Y. Pouillon, R. Caracas, F. Jollet, M. Torrent, G. Zerah, M. Mikami *et al.*, Z. Kristallogr. **220**, 558 (2005).
[24] M. Fuchs and M. Scheffler, Comput. Phys. Commun. **119**, 67 (1999).
[25] N. Troullier and J. L. Martins, Phys. Rev. B **43**, 1993 (1991).
[26] H. J. Monkhorst and J. D. Pack, Phys. Rev. B **13**, 5188 (1976).
[27] M. Bernasconi, G. L. Chiarotti, and E. Tosatti, Phys. Rev. B **52**, 9988 (1995).
[28] Y. Takao and A. Morita, Phys. B **105**, 93 (1981).
[29] V. Kumar and B. S. R. Sastry, Phys. Stat. Sol. **242**, 869 (2005).
[30] T. Wedsten, Acta Chem. Scand. **21**, 1374 (1967).
[31] F. Bachhuber, J. Rothballer, F. Pielnhofer, and R. Weihrich, J. Chem. Phys. **135**, 124508 (2011).
[32] O. Romanyuk, F. Grosse, and W. Braun, Phys. Rev. B **79**, 235330 (2009).
[33] O. Romanyuk, F. Grosse, and W. Braun, Phys. Status Solidi C **7**, 330 (2010).
[34] R. G. Dandrea, S. Froyen, and A. Zunger, Phys. Rev. B **42**, 3213 (1990).
[35] O. Romanyuk, V. M. Kaganer, R. Shayduk, B. P. Tinkham, and W. Braun, Phys. Rev. B **77**, 235322 (2008).
[36] M. E. Lazzouni, M. Peressi, and A. Baldereschi, Appl. Phys. Lett. **68**, 75 (1995).
[37] Che Jingguang, Zhang Kaiming, and Xie Xide, Phys. Rev. B **50**, 18167 (1994).
[38] C. Huang, L. Ye, and X. Wang, J. Phys. Condens. Matter **1**, 907 (1989).